Target effects in the interaction of highly charged Ne ions with an Al(110) surface

S. Hustedt, J. Freese, S. Mähl, and W. Heiland
Fachbereich Physik, Universität Osnabrück, Barbarastraße 7, D-49069 Osnabrück, Germany

S. Schippers
Kernfysisch Versneller Instituut, Zernikelaan 25, NL-9747 AA Groningen, The Netherlands

J. Bleck-Neuhaus
Fachbereich Physik, Universität Bremen, Kufsteiner Straße 1, D-28359 Bremen, Germany

M. Grether, R. Köhrbrück, and N. Stolterfoht
Hahn-Meitner-Institut Berlin, Glienicker Straße 100, D-14109 Berlin, Germany
and Laboratoire de Spectroscopie Atomique, Institut des Sciences de la Matière et du Rayonnement, Campus II, F-14040 Caen Cedex, France
(Received 16 May 1994)

We studied the potential electron emission arising from the interaction of H-like Ne^{9+} ions with clean Al(110) and Pt(110) surfaces at different glancing angles (10°–90°) with 90-keV impact energy. Projectile KLL Auger electrons are found to be emitted from inside the solid. Therefore, the measured electron energy distributions are influenced by solid-state effects. We present a deconvolution procedure to determine the scattering contribution to the measured spectra for Al targets. After a subtraction of the scattering contribution we compare the resulting primary emission spectra with atomic structure calculations. The calculations show that at the moment of KLL Auger electron emission the projectile L shell is completely filled for an Al target, whereas for a Pt target there were on the average only five electrons in the projectile L-shell. This indicates a relatively faster L-shell filling process for Al targets.

PACS number(s): 79.20.Nc, 61.80.Mk

I. INTRODUCTION

During the past few years the interaction of slow highly charged ions with clean metal surfaces has been studied intensively. A major tool is angular and energy resolved electron spectroscopy [1–11]. A well accepted picture for the neutralization process of the ions in front of and inside the surface is the following. Starting at rather large distances from the surface, the ions capture electrons from the metal conduction band into highly excited projectile states with high principal quantum numbers, forming so called "hollow atoms." For example for Ne^{9+} these quantum numbers are $9 \leq n \leq 11$. The distance of formation of the hollow atoms above the surface can be estimated by applying the "over-the-barrier" model for resonant electron exchange between metal and projectile [12]. For Ne^{9+} ions and Al and Pt targets this distance is about 12 Å. Subsequently to the direct resonant filling of electrons in outer projectile states a deexcitation cascade starts, filling stepwise the projectile vacancies in inner shells from the outer projectile states and from target states.

Of special interest are the time scales for the different processes involved in the neutralization of the projectile, especially the L- and K-Auger processes filling the innermost shells, and the charge distribution among the different shells during these processes. The question of whether these processes occur in front of or inside the surface has been investigated in detail. Depending on the projectile's velocity "above" surface [4,5,9] and "below" surface [2,4,5,8,10,11] deexcitation has been observed.

Here we investigate the electron emission from 90-keV Ne^{9+} ions interacting with an Al(110) single crystal surface. For a Pt target we have shown previously that the Ne K-shell vacancies survive the transport to the surface and that they are filled by K-Auger processes below the surface [10,11].

Our present experiments with an Al target reveal also a K-Auger emission from inside the solid. Therefore, our electron energy distributions are distorted by elastic and inelastic electron scattering processes inside the solid. It has been shown that after subtraction of the so called scattering contribution [13], the measured energy distributions of the projectile K-Auger electrons agree with results of atomic structure calculations. A deconvolution procedure for transition metal targets has previously been presented [10]. Here we present now a deconvolution procedure for Al targets. Due to the different electronic properties of transition metals and "jellium" metals like Al the electron energy loss cross section is different for the two types of targets. This results in different shapes and energetic shifts in the measured K-Auger electron spectra for Al and Pt.

For comparison with calculated electron energy distributions, we separated the inelastic contributions from the measured spectra. The analysis leads to the deter-

mination of the electron distribution over the projectile shells at the instant of K-Auger electron emission. In the case of $10q$-keV N^{6+}, O^{7+}, and Ne^{9+} impinging onto a Pt(110) surface under a glancing angle of $\psi = 10°$, there are on the average 5 L electrons present at the instant of K-Auger electron emission [10]. This result will be compared to the results for an Al target.

II. EXPERIMENT

The experiments were performed at the 14.4 GHz electron cyclotron resonance (ECR) ion source at the Hahn–Meitner-Institut in Berlin. Inside a μ-metal ultrahigh-vacuum (UHV) chamber specially designed for energy- and angle-resolved electron spectroscopy a monocrystalline Al(110) target was mounted on a two axes goniometer. The glancing angle was varied from $\psi = 10°$ to 90°. With respect to the crystallographic directions a "random" azimuthal angle was chosen, in order to minimize channeling effects. A tandem parallel plate electron energy analyzer [14] allows for the measurement of angular-resolved energy spectra in an angular range of $0° < \theta \leq 180°$ with respect to the incident beam direction. The electron observation angle θ was varied from 10° to 140°. The energy resolution of the spectrometer was $\Delta E/E = 2.5\%$.

Inside the chamber the target can be prepared by sputter cleaning and electron beam heating and its surface can be characterized by Auger electron spectroscopy (AES), ion scattering spectroscopy, and low energy electron diffraction. The base pressure during the experiment was 1×10^{-10} mbar. A 140-nA mass- and charge-selected beam of 90 keV Ne^{9+} was collimated to a diameter of 2 mm before entering the chamber.

The measured doubly differential electron energy distributions were normalized to an absolute scale, taking into account geometrical effects, the spectrometer transmission, and the detection efficiency. For details concerning the normalization procedure see Refs. [7,15,16].

III. RESULTS

The following analysis of measured electron energy distributions clearly shows a projectile K-Auger electron emission from inside the surface.

Figure 1 shows the normalized electron energy distributions for $10q$-keV Ne^{q+} ($q = 8, 9, 10$), impinging under $\psi = 10°$ on the Al(110) surface. The detection angle was $\theta = 40°$. Note that the electron yield scale is logarithmic. The exponentially decreasing background is due to kinetic electron emission. The structure at 140 eV can be attributed to Ne-L-Auger processes, filling the L shell of the projectile. The broad structure ranging from 200 eV up to 1400 eV for Ne^{9+} and Ne^{10+} originates from Auger processes, filling the Ne-K shell [10]. For Ne^{8+} this structure is strongly reduced because there is only a small fraction of metastable Ne^{8+} ions (with a K shell vacancy) in the beam. For Ne^{9+} there is one peak, representing the filling of the K-shell vacancy via

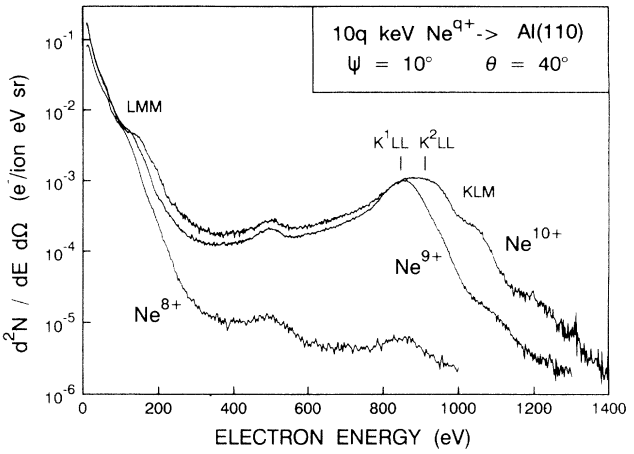

FIG. 1. Angular- and energy-resolved electron spectra of 80-keV Ne^{8+}, 90-keV Ne^{9+}, and 100-keV Ne^{10+} interacting with an Al(110) surface for glancing angle $\psi = 10°$ and electron observation angle $\theta = 40°$. The spectra are corrected for spectrometer transmission, the yield scale is logarithmic. The structure at 500 eV is due to a small O contamination. The Ne LMM Auger peak shifts to higher energies for higher charge states, the KLL Auger peak for Ne^{10+} has a double structure, originating from the filling of the first and second K-shell vacancy (K^2LL and K^1LL Auger transitions).

a KLL Auger process. In the case of Ne^{9+} and Ne^{10+} there are shoulders on the high energy side of the energy distributions, originating from K-Auger processes involving higher shells of the projectile, e.g., KLM and KMX Auger transitions. For Ne^{10+} the maximum has a double peak structure, originating from the subsequent filling of the two K-shell holes. The K-Auger structures for Ne^{9+} and Ne^{10+} have a long tail on the low energy side. This is due to K-Auger electrons which have lost a certain amount of their kinetic energy by inelastic scattering events inside the solid. Thus the primary electron emission spectra are distorted by solid state effects.

In Fig. 2 the normalized electron spectra for 90-keV Ne^{9+} interacting with an Al(110) surface are shown. The kinetic background has been subtracted. With fixed detection angle at $\theta = 120°$ the angle of incidence was varied from $\psi = 10°$ to 90°. The spectra are transformed to the projectile's rest frame. The substructure at the low energy side can be attributed to a small oxygen contamination which could not be totally removed from the surface. It is only apparent at small angle of incidence. Therefore, we conclude that the oxygen contamination is confined only to the topmost surface layer. For our experiment with rather high energies ($v \simeq 0.5$ a.u.) this small oxygen contamination is not expected to disturb our analysis.

There are two obvious features in the spectra: with increasing angle of incidence the position of the peak maximum is shifted to lower energies and the peak intensity decreases. The inset shows the integrated K-Auger peak area versus angle of incidence. The area is exponentially decreasing with increasing angle of incidence. The energetic position of the KLL peak shifts

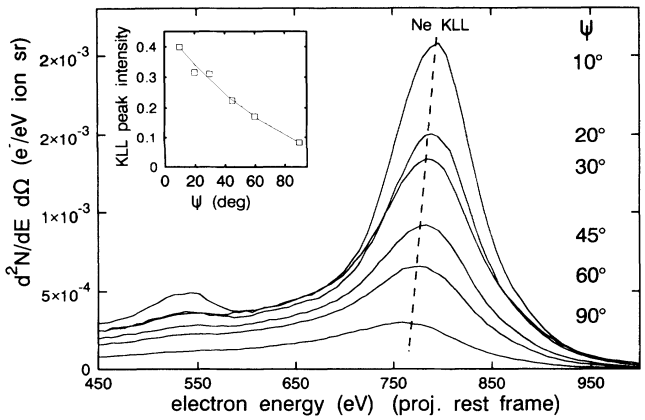

FIG. 2. Variation of the Ne-K-Auger peak with varying glancing angle ψ for 90-keV $Ne^{9+} \rightarrow Al(110)$. The electron observation angle is $\theta = 120°$. The spectra are kinetic background subtracted and corrected for the spectrometer transmission. The maximum of the K-Auger peak is shifted to lower energies and the electron yield decreases (see inset) when the glancing angle ψ is increased.

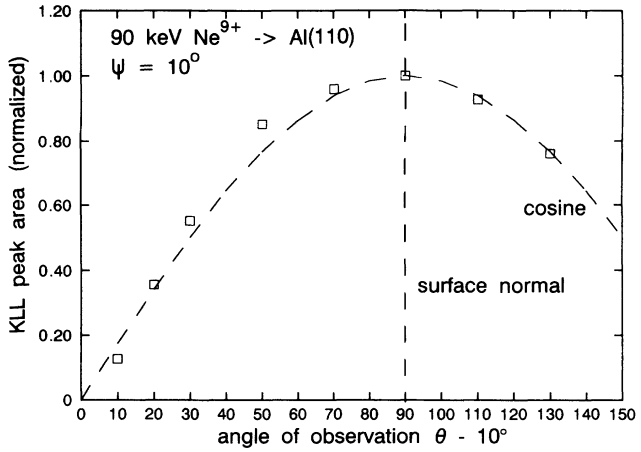

FIG. 4. Variation of the Ne-K-Auger peak area with varying angle of observation Θ (squares). The direction of the surface normal was set to $\Theta = 90°$, the angle of incidence is $\psi = 10°$, so $\Theta = \theta - 10°$. The datapoints can be fitted by a pure cosine distribution (dashed line).

from 792 eV for $\psi = 10°$ to 760 eV for $\psi = 90°$. These are clear indications for an electron emission from inside the solid: For increasing angles of incidence the ions penetrate deeper into the solid until the electron emission takes place. Electrons that are emitted from deeper layers inside the solid undergo more elastic and inelastic scattering events with the solid before they can escape from the surface (and enter the detector). This results in a larger energy loss and a general decrease of the electron yield for increasing angle of incidence.

In Fig. 3 the Ne^{9+}-K-Auger peak is shown for fixed angle of incidence $\psi = 10°$, the observation angle was varied from 10° to 140°. The peak maximum shifts to lower energies for larger observation angles due to electron emission from the moving projectile. The electron yield is largest for $\theta = 100°$, i.e., in case of observation normal to the surface. At other observation angles electron trajectories inside the solid on the average are longer. The corresponding increased number of scattering events inside the solid leads to an attenuation of the electron into the vacuum.

Figure 4 shows the integrated Ne-K-Auger peak area versus angle of observation. The yield was normalized at $\theta = 100°$ to unity. The dashed line is a cosine distribution. The cosine distribution is expected for an electron emission from inside the solid. The agreement between the experimental data and the cosine distribution is very good.

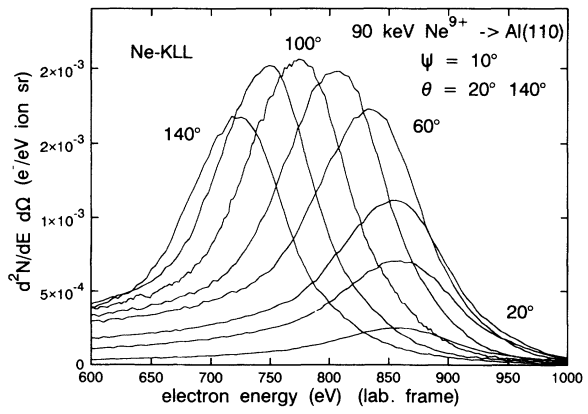

FIG. 3. Electron spectra from 90-keV Ne^{9+} interacting with an Al(110) surface. The angle of incidence was $\psi = 10°$, the observation angle was varied from $\theta = 20°$ to $\theta = 140°$. With increasing observation angle the structures shift to lower energies. This is a kinematic effect, the electrons are emitted from a moving projectile. The maximum yield is at $\theta = 100°$, which represents the surface normal.

IV. DECONVOLUTION OF THE PRIMARY SPECTRUM

As mentioned above the projectile K-Auger electron emission for 90-keV Ne^{9+} on Al(110) takes place inside the solid. This situation is similar to x-ray photoelectron spectroscopy (XPS) and Auger electron spectroscopy (AES). Also in XPS and AES the primary excitation spectra are modified by elastic and inelastic electron scattering inside the solid. In order to use XPS and AES for quantitative surface chemical analysis, the primary excitation spectrum $F(E)$ has to be determined from the measured distorted electron spectrum $j(E)$. This task is done in the most appropriate way by using the deconvolution procedure developed by Tougaard [17]. It was found [18] that the in-depth distribution of K-Auger electron emission arising from the interaction of highly charged ions with solid surfaces is an exponential like in XPS. The exponential is due to the lifetime of the K-shell holes in the projectile, i.e., the number of K-shell holes in the flux of penetrating projectiles decreases

exponentially with the depth. With this type of in-depth distribution, i.e.,

$$f(x) = c\exp(-x/L_a),$$

we have

$$F(E) = j(E) - \frac{\lambda L_a}{\lambda\cos\alpha + L_a}\int_E^\infty K(E'-E)j(E')\mathrm{d}E', \tag{1}$$

where λ is the inelastic mean free path, L_a is the attenuation length, and α is the exit angle with respect to the surface normal. For transition metals, the universal cross section $\lambda K(E'-E)$ is

$$\lambda K(E'-E) \cong \frac{B(E'-E)}{[C+(E'-E)^2]}, \tag{2}$$

with $B \cong 2866$. With (2) the primary spectrum is

$$\begin{aligned} F(E) &= j(E) - S(E) \\ &= j(E) - B_1\int_E^\infty \frac{E'-E}{[C+(E'-E)^2]^2}j(E')\mathrm{d}E', \end{aligned} \tag{3}$$

where C is fixed at 1643 eV^2 and B_1 is used as a fit parameter. It is chosen in a way that the calculated scattering contribution fits to the low energy end of the peak of interest as shown in Ref. [10]. Due to the fact that the K-Auger electrons are emitted from a *moving* projectile the application of Eq. (1) is restricted to spectra which have been recorded under small electron observation angles, i.e., $\theta < 90°$. Details have been worked out elsewhere [10,13,19].

The electronic structure of Al ("jellium" metal) is quite different from transition metals, so the dielectric response function and correspondingly the inelastic cross section for Al have a different shape. We base our calculation of the scattering contribution for Al targets on the approximation of the dielectric response function and inelastic cross section described in Ref. [20].

The inelastic cross section $K(E,\omega)$ can be written in the following way:

$$K(E,\omega) = \frac{1}{\pi E}\int_{q_-}^{q_+}\frac{dq}{q}\mathrm{Im}\left\{\frac{-1}{\epsilon(q,\omega)}\right\}, \tag{4}$$

where $E = v^2/2$ is the energy of the electron, v is the electron velocity, $\omega = E'-E$ is the energy loss, and the limits of the integration over momentum transfer q are given by $q_\pm = v \pm \sqrt{v^2-2\omega}$ (in atomic units). The data for the imaginary part of the dielectric function were taken from optical measurements [21]. The optical data were approximated by a Drude-type function (energy 15.06 eV, width 0.54 eV) and Eq. (4) was solved numerically. An earlier published analytical solution of the above formula [22] was found to be incorrect.

The dominant interaction of the fast Auger electrons with the target electrons will be in form of plasmon excitations. To take the surface plasmon interactions into account we introduced a second Drude-type function (energy 10.65 eV, width 0.54 eV) representing the surface plasmon contribution. For the energetic position of the surface plasmon contribution the bulk plasmon energy was scaled with $1/\sqrt{2}$ and we assumed the same energy width. The relative intensities of the two contributions were determined by deconvoluting the scattering contribution from experimental Al XPS data, using the inelastic cross section as resulting from Eq. (4).

The best fit is shown in Fig. 5. The intensity ratio between the surface and bulk plasmon contribution was 1:7. The deconvoluted scattering contribution fits nicely the background due to multiple plasmon excitations. There

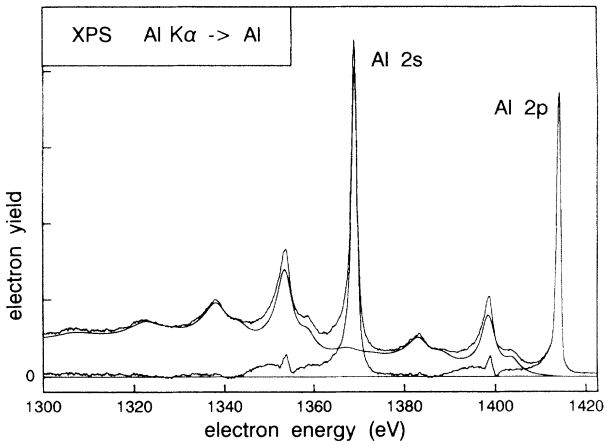

FIG. 5. Experimental Al $K\alpha$-excited photoelectron spectrum from pure aluminium (upper curve) and the primary excitation spectrum as determined by (1) and (4) (lower curve). The difference curve is the background signal of the inelastically scattered electrons. The fit parameter are $\omega_{0s} = 10.4$ eV, $\omega_{0b} = 15.5$ eV, $\gamma_s = 3$ eV, $\gamma_b = 3$ eV, $A_s = 4.6$, and $A_b = 4.6$. The Al-$K\alpha$ line (1486.7 eV) was monochromatic, full width at half maximum 0.2 eV.

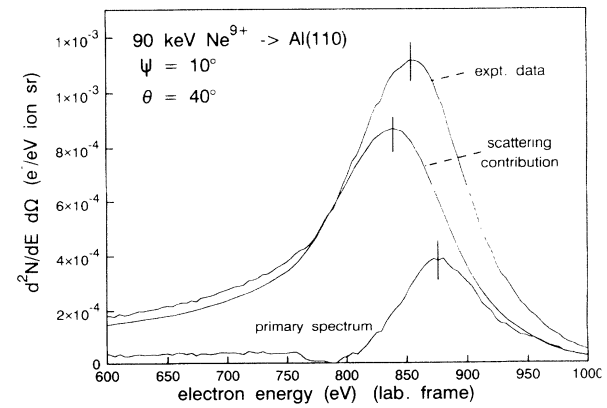

FIG. 6. An example for deconvolution of the scattering contribution from a measured electron energy distribution [90-keV Ne^{9+} on Al(110), $\psi = 10°$, $\theta = 40°$]. Shown is the Ne-K-Auger structure in the lab rest frame after subtraction of the kinetic background and normalization. The "Tougaard background" was fitted to the low energy side of the spectrum. The lower curve is the resulting primary excitation spectrum. Its maximum is shifted towards higher energies.

are small discrepancies between experiment and fitted scattering contribution because not all interactions are included in the Tougaard model, but this has only minor influence on our analysis of measured electron spectra from highly charged ion-surface interactions. For experimental details see the caption of Fig. 5.

Having determined the inelastic cross section in this way the scattering contribution was deconvoluted from our measured Ne-K-Auger spectra on Al. It was performed in a way that the calculated scattering contribution fits to the low energy end of the peak of interest as shown in Fig. 6. Monte Carlo simulations of electron emission from inside a solid show comparable results concerning the shape of the scattering contribution. The position of the maximum of the measured electron energy distribution is at 853 eV, after subtraction of the scattering contribution it is at about 875 eV (in the laboratory rest frame). For a Pt target with the same experimental parameters this shift, resulting from the background subtraction, is from 832 eV to 858 eV.

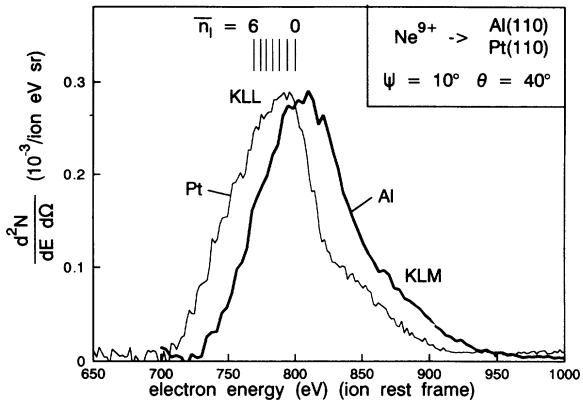

FIG. 7. Comparison between the energetic position of measured and calculated Ne-K-Auger electron energy spectra. The thick solid line is the measured spectrum ($\psi = 10°, \theta = 40°$) for the Al target, the thin solid line for the Pt target. For comparison the Pt spectrum is normalized to the height of the Al spectrum, both spectra are shown in the projectiles rest frame after subtraction of the target specific Tougaard scattering contributions, respectively. The vertical lines indicate the centroid energy of the calculated distributions (Cowan computer code [24]). Variation parameter for the calculations was the number of L-shell vacancies $\bar{n}_l$ at the moment of K-Auger electron emission. One electron was in the K shell, the M shell was filled up to neutrality. The measured spectrum for Al agrees best with the calculated position under the assumption that at the instant of emission of the KLL-Auger electron the L-shell is completely filled ($\bar{n}_l = 0$), whereas for Pt the measured spectrum agrees best with the calculated line for three vacancies in the projectile L shell ($\bar{n}_l = 3$). This we find for all angles of observation.

V. DISCUSSION

The primary excitation spectrum $F(E)$ obtained after subtraction of the Tougaard scattering contribution $S(E)$ contains information about the neutralization dynamics of the projectile. The deexcitation of the hollow atom proceeds in several steps. The K-Auger processes filling the projectile K holes are to be considered as the final step of the deexcitation cascade. They cannot proceed before electrons have been filled into the projectile L shell by previous steps. For a KLM-Auger or a KLL-Auger process at least 1 or 2 L electrons are required, respectively. The number of L electrons present at the instant of K Auger electron emission is usually not known, because it depends on the complex dynamics of all previous neutralization and deexcitation steps. However, the energy distribution of the K Auger electrons depends on the distribution of the electrons among the projectile shells at the instant of K Auger electron emission [23].

As described before we performed atomic structure calculations of projectile Auger electron energy spectra in order to determine the electron distribution [10,19] using the conıputer code of Cowan [24]. Within the atomic structure calculations, we estimate the electron distribution among the projectile shells prior to the Auger process. Especially the number n_l of projectile L holes is varied. Within the calculations we always assume that the projectile is neutral prior to the Auger process of interest, i.e., in the Ne case the projectile M shell contains the remaining electrons because it can be argued that the M shell is the highest existing Ne shell inside the solid [25].

The comparison between measured (after subtraction of the scattering contribution and transformation into the projectile's rest frame [10]) and calculated K-Auger electron spectra is shown in Fig. 7 for the Al and Pt targets. The vertical bars indicate the average energetic position of the calculated KLL Auger structures. From the comparison with our experimental data for Al (thick solid line), we conclude that the Ne-L shell is completely filled at the moment of the KLL-Auger electron emission. For the Pt target the energetic position of the measured spectrum best fits the calculated position for three projectile L-shell vacancies, so the Ne-K-shell vacancies are filled via K-Auger processes before the Ne-L shell is completely filled. We obtain the same result for all angles of observation.

This indicates a much stronger electronic interaction between the projectile and the solid in the case of Al. Thus, the L-shell filling apparently proceeds faster in Al than in Pt. Under comparable conditions we obtained the same result, e.g., a completely filled projectile L shell in the moment of the K-Auger transition for hydrogenlike N on Al(110) [26]. This finding could be explained in the following way.

As stated above, the projectile M shell is assumed to be filled instantaneously when the projectile enters into the solid. Now a deexcitation cascade starts, filling the projectile L and K shell subsequently via L and K Auger processes. The intra-atomic L- and K- Auger transition rates should be rather independend of the solid. Of more importance is the "side-feeding" process as introduced by Ref. [1], a direct resonant filling mechanism of valence

band electrons into the projectile L shell. This process depends strongly on the projectile velocity, the target atom density and the number of free electrons per atom in the target. The more atoms are passed by per unit time and the higher the free electron density, the higher may be the probability of capturing an electron into the projectile L-shell.

In our experiments the projectile velocity was kept constant and the atomic densities of Al and Pt are nearly equal, but the free electron density of Al ("jellium metal") is three times larger than for Pt (transition metal with strongly localized d electrons). So in a very simple model the "side-feeding"-transition rate should be three times larger in Al than in Pt.

We conclude that the differences in the electronic structure of Al as compared to Pt fosters faster neutralization of the highly charged projectiles. Further details about the electron emission arising from the interaction of 90-keV Ne^{9+} and 100-keV Ne^{10+} ions on an Al(110) target will be presented elsewhere [26].

VI. CONCLUSIONS

We studied the electron emission from highly charged Ne ions interacting with Al(110) and Pt(110) surfaces. It could be shown that the Ne-K-Auger electron emission takes place inside the solid, e.g., the inner shell vacancies survive the transport to the surface. We presented an algorithm for deconvoluting the contribution due to elastic and inelastic scattering events inside the solid from our measured electron energy distibutions. This allows a comparison of the primary excitation spectra with calculated electron energy distributions. The comparison provides detailed insight in the neutralization dynamics of the highly charged ions at the metal surface. For the Al target, we find that at the moment of K-Auger electron emission the L shell is completely filled, whereas for a Pt target there is a number of three L-shell vacancies reported at the moment of K-Auger electron emission [10]. This is a strong indication for a relatively fast L-shell filling process in Al.

ACKNOWLEDGMENTS

We gratefully acknowledge the generous assistance of the staff of the HMI ECR source. We thank A. Arnau, P. Echenique (San Sebastian), and R. Morgenstern (Groningen) for helpful discussions. This research was supported in part by the Bundesministerium für Forschung und Technologie, by the Deutscher Akademischer Auslandsdienst (DAAD) and the European Union (HCM project).

[1] L. Folkerts and R. Morgenstern, Europhys. Lett. **13**, 377 (1990).
[2] J. P. Briand, L. de Billy, P. Charles, S. Essabaa, P. Briand, R. Geller, J. P. Desclaux, S. Bliman, and C. Ristori, Phys. Rev. Lett. **65**, 159 (1990).
[3] P. A. Zeijlmans van Emmichoven, C. C. Havener, and F. W. Meyer, Phys. Rev. A **43**, 1405 (1991).
[4] F. W. Meyer, S. H. Overbury, C. C. Havener, P. A. Zeijlmans van Emmichoven, and D. M. Zehner, Phys. Rev. Lett. **67**, 723 (1991); F. W. Meyer, S. H. Overbury, C. C. Havener, P. A. Zeijlmans van Emmichoven, J. Burgdörfer, and D. M. Zehner, Phys. Rev. A **44**, 7214 (1991).
[5] H. J. Andrä, A. Simionovici, T. Lamy, A. Brenac, G. Lamboley, J. J. Bonnet, A. Fleury, M. Bonnefoy, M. Chassevent, S. Andriamonje, and A. Pesnelle, Z. Phys. D **211**, S135 (1991); H. J. Andrä, A. Simionovici, T. Lamy, A. Brenac, G. Lamboley, A. Presnelle, S. Andriamonje, A. Fleury, M. Bonnefoy, M. Chassevent, and J. J. Bonnet, in *Electronic and Atomic Collisions*, edited by W. R. MacGillivray, I. E. McCarthy, and M. C. Standage, (Adam Hilger, Bristol, 1992), p. 89.
[6] R. Köhrbrück, K. Sommer, J. P. Biersack, J. Bleck-Neuhaus, S. Schippers, P. Roncin, D. Lecler, F. Fremont, and N. Stolterfoht, Phys. Rev. A **45**, 4653 (1992).
[7] S. Schippers, S. Hustedt, W. Heiland, R. Köhrbrück, J. Bleck-Neuhaus, J. Kemmler, D. Lecler, and N. Stolterfoht, Phys. Rev. A **46**, 4003 (1992).
[8] J. Das, L. Folkerts, and R. Morgenstern, Phys. Rev. A **45**, 4669 (1992).
[9] J. Das and R. Morgenstern, Phys. Rev. A **47**, R755 (1993).
[10] S. Schippers, S. Hustedt, W. Heiland, R. Köhrbrück, J. Bleck-Neuhaus, J. Kemmler, D. Lecler, and N. Stolterfoht, Nucl. Instrum. Methods Phys. Res. Sect. B **78**, 106 (1993).
[11] R. Köhrbrück, S. Hustedt, S. Schippers, W. Heiland, J. Bleck-Neuhaus, J. Kemmler, D. Lecler, and N. Stolterfoht, Nucl. Instrum. Methods Phys. Res. Sect. B **78**, 93 (1993).
[12] J. Burgdörfer and F. W. Meyer, Phys. Rev. A **47**, R20 (1993).
[13] J. Bleck-Neuhaus, R. Page and A. Saal, Nucl. Instr. Methods Phys. Res. Sect. B **78**, 113 (1993).
[14] A. Itoh, T. Schneider, G. Schiwietz, Z. Roller, H. Platten, G. Nolte, D. Schneider, and N. Stolterfoht, J. Phys. B **16**, 3965 (1983).
[15] R. Köhrbrück, Ph. D. thesis, Technische Universität Berlin, 1992.
[16] R. Köhrbrück, N. Stolterfoht, S. Schippers, S. Hustedt, W. Heiland, D. Lecler, J. Kemmler, and J. Bleck-Neuhaus, Phys. Rev. A **48**, 3731 (1993).
[17] S. Tougaard, Surf. Sci. **216**, 343 (1989).
[18] S. H. Overbury, F. W. Meyer, and M. T. Robinson, Nucl. Instrum. Methods Res. Sect. B **67**, 126 (1992).
[19] S. Schippers, Ph.D. thesis, Universität Osnabrück, 1992.
[20] S. Tougaard and I. Chorkendorff, Solid State Commun. **57**, 77 (1986).

[21] *Handbook of Optival Constants of Solids*, edited by E. D. Palik (Academic Press, New York, 1985).
[22] J. C. Ashley, J. J. Cowan, R. H. Ritchie, V. E. Anderson, and J. Hoelzl, Thin Solid Films **60**, 361 (1979).
[23] N. Stolterfoht, Phys. Rep. **146**, 315 (1987).
[24] R. D. Cowan, *The Theory of Atomic Structure and Spectra* (University of California Press, Berkeley, 1981).
[25] J. Burgdörfer, in *High-Energy Ion-Atom Collisions, Lecture Notes in Physics* (Springer-Verlag, Berlin, 1991), Vol. 376, p. 199.
[26] S. Hustedt, J. Freese, W. Heiland, M. Grether, J. Limburg, R. Hoekstra, and R. Morgenstern (unpublished).